

## Key Points:

- Models with realistic Congo rainfall simulate higher rainfall in November, the peak of the second wet season, than March, the peak of the first
- Models with realistic Congo evaporation simulate lower evaporation in November than March, because these models suppress transpiration
- Using subgrid rainfall schemes in all global climate models could improve how models produce Congo evaporation during the wet seasons

## Correspondence to:

D. M. Crowhurst,  
david.crowhurst@ouce.ox.ac.uk

## Citation:

Crowhurst, D. M., Dadson, S. J., & Washington, R. (2020). Evaluation of evaporation climatology for the Congo Basin wet seasons in 11 global climate models. *Journal of Geophysical Research: Atmospheres*, 125, e2019JD030619. <https://doi.org/10.1029/2019JD030619>

Received 12 MAR 2019

Accepted 31 JAN 2020

Accepted article online 3 FEB 2020

© 2020. The Authors.

This is an open access article under the terms of the Creative Commons Attribution License, which permits use, distribution and reproduction in any medium, provided the original work is properly cited.

## Evaluation of Evaporation Climatology for the Congo Basin Wet Seasons in 11 Global Climate Models

David M. Crowhurst<sup>1</sup> , Simon J. Dadson<sup>1</sup> , and Richard Washington<sup>1</sup> 

<sup>1</sup>School of Geography and the Environment, University of Oxford, Oxford, UK

**Abstract** Across the Congo, there is a wide spread in rainfall in the two wet seasons in Coupled Model Intercomparison Project 5 global climate models (GCMs). As the Congo is believed to be a moisture recycling hot spot, the evaporation of excess water from the land surface in some models could be amplifying the model spread in rainfall. This study performs an exploratory process-based evaluation of Congo Basin evaporation in 11 Coupled Model Intercomparison Project 5 GCMs that took part in the Atmospheric Model Intercomparison Project. Our aims are to improve scientific understanding about Congo evaporation, and to determine whether there are opportunities to improve how models produce Congo evaporation. Climatologically, we find that models with “realistic” rainfall simulate higher rainfall in November, the peak of the second wet season, than March, the peak of the first. However, models with “realistic” evaporation simulate lower evaporation in November than March, because these models suppress the transpiration component of the evaporation in November relative to March. In both wet seasons, subgrid rainfall schemes make these models simulate a credible ratio of transpiration to canopy evaporation, and cause them to generate evaporation in a more realistic manner. We therefore trust how these models produce evaporation in the wet seasons, and argue that lower transpiration is likely to explain why evaporation is lower in November than March in reality. We also suggest that using subgrid rainfall schemes in all GCMs could improve how models produce Congo evaporation during the wet seasons. This might reduce the model spread in Congo rainfall.

## 1. Introduction

The Congo Basin is one of three major global hot spots of convective rainfall (Webster, 1983). Congo climate is of critical global importance, as latent heat release drives the large-scale tropical and subtropical circulation, delivering heat and moisture poleward (Jury & Mpeta, 2009). Regionally, Congo climate is important given the sensitivity of agriculture to rainfall (Sonwa et al., 2017). Furthermore, the Congo Basin rainforests and the peatlands beneath them are a particularly large store of carbon (Dargie et al., 2017; Xu et al., 2017), and the release of carbon due to either deforestation or peatland decomposition is a significant threat (Dargie et al., 2018). Unfortunately, there is currently a wide spread in global climate model (GCM) simulations of Congo Basin rainfall amount and distribution during the two wet seasons, which have peak rainfall in March and November (Haensler et al., 2013). As the models differ vastly in their simulation of present-day wet season rainfall, credibility in model projections of future rainfall is undermined. This problem is hampering the development of adaptation strategies for the Congo Basin, which are required to lessen vulnerability to changes in rainfall (Bele et al., 2015). In addition, it is not yet possible to work out whether the Congo Basin will have water stress during the wet seasons (Zhou et al., 2014). To resolve this, it is essential to establish whether some models produce realistic and credible simulations of Congo Basin rainfall in the wet seasons, as these models are more likely to have trustworthy projections. In addition, if certain model schemes are responsible for improving model rainfall, these schemes could be used more widely to reduce the model spread.

Washington et al. (2013) were the first to identify the wide spread in rainfall amount and distribution in the Congo Basin wet seasons in coupled GCMs from the fifth phase of the Coupled Model Intercomparison Project (CMIP5). Building upon this, Creese and Washington (2016) suggested that an observational campaign at key Congo Basin boundaries could help to constrain the spread in model rainfall. Furthermore, Creese and Washington (2018) argued that models with large sea surface temperature (SST) biases in the Gulf of Guinea produce more evaporation from the ocean, enhanced local convection, and higher rainfall in the western Congo Basin during the September–October–November rainy season. Their results questioned

the credibility of Congo Basin rainfall produced by models with large Atlantic SST biases. Nevertheless, in CMIP5 models participating in the Atmospheric Model Intercomparison Project (AMIP) experiment, where observed SST is prescribed and SST biases cannot account for model differences in rainfall, there is still a wide spread in rainfall amount during the two wet seasons in the Congo Basin. A potential reason for the remaining spread is that errors in model land surface schemes could cause models to generate divergent evaporation from the land surface in response to a unit of rainfall. As evidence from moisture tagging algorithms indicates that the Congo Basin is a hot spot of moisture recycling (Dyer et al., 2017; Pokam et al., 2012), it is possible that the release of excess water vapor from the land surface through evaporation (often referred to as “evapotranspiration”) in some models could be amplifying the model spread in Congo Basin rainfall.

### 1.1. Process-Based Evaluation of Congo Basin Evaporation

This study performs an exploratory process-based evaluation of Congo Basin evaporation for a selection of CMIP5 GCMs which took part in AMIP. Process-based evaluation methods establish whether models reproduce reference data well (with “realism”), using a physically credible set of processes (James et al., 2018). The purpose of this evaluation is twofold. The first is to improve scientific understanding about the annual cycle of evaporation and its three components, canopy evaporation, transpiration, and soil evaporation, in the Congo Basin. If some models realistically simulate evaporation against reference data, and partition evaporation into its components using credible processes, this would strengthen the trustworthiness of their evaporation partitioning. The three components of evaporation produced by these models could then provide some information about why the annual cycle has the characteristics that it does, in the absence of in situ data for these components in the Congo Basin. The second purpose is to identify methods to improve how Congo Basin evaporation is generated in the GCMs. Certain GCMs might contain favorable schemes within their land surface models (LSMs) which credibly alter the partitioning of evaporation to bring evaporation into good agreement with reference data. If some GCMs contain favorable schemes, while others do not, this would present an opportunity to improve how models simulate Congo Basin evaporation, by using favorable schemes more widely. This might contribute to reducing the model differences in Congo Basin rainfall in the wet seasons.

### 1.2. Aims

This study aims to answer the following questions:

1. How is evaporation partitioned into its components in the Congo Basin in GCMs with more “realistic” evaporation, and what can this tell us about the evaporation?
2. Are there opportunities to improve the realism of Congo Basin evaporation across GCMs?

In section 2, we describe the data and methods used. In section 3, we compare the annual cycle of evaporation produced by a range of GCMs against reference data, and establish what defines the annual cycle for models which have more realistic evaporation than others. In section 4, we determine how evaporation is partitioned into its three components in these models, and assess the credibility of the processes which do this. If the evaporation is plausibly produced, we will be able to use the model evaporation partitioning to gain some useful information about the characteristics of the evaporation. In section 5, we discuss the results, and in section 6, we conclude.

## 2. Data and Methods

### 2.1. Domain

The Congo Basin domain is defined as 14°S to 4°N, 18°E to 29°E (Figure 1). Although the Congo Basin has evergreen rainforests to the north and deciduous savannah to the south (Yan et al., 2017), we select the whole Congo Basin to complement previous process-based rainfall (Creese & Washington, 2018) and water vapor transport (Pokam et al., 2012) analyses. No study has done the same for evaporation. By considering the entire Congo Basin, the current exploratory study begins to improve knowledge about evaporation and its three components for the region as a whole.

### 2.2. AGCMs

This study focuses on monthly thirty-year mean (1979–2008) atmosphere-only global climate model (AGCM) simulations from the AMIP component of CMIP5 (Taylor et al., 2012). AMIP simulations are preferred

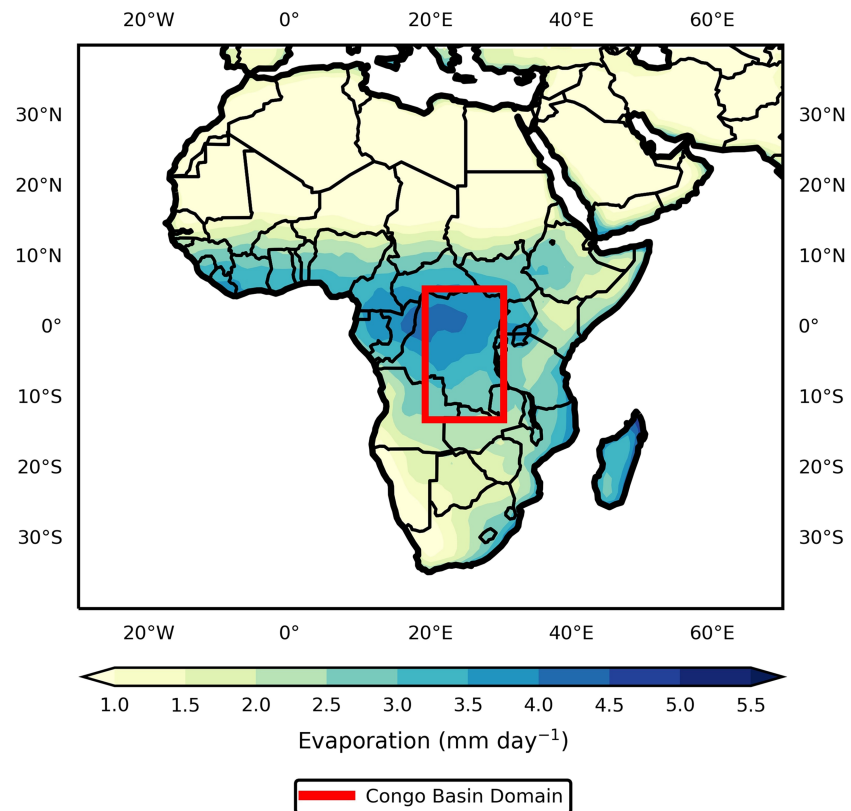


**Figure 1.** Thirty-year mean (1979–2008) evaporation across the African continent ( $\text{mm day}^{-1}$ ), from a composite mean of the 11 AMIP models used in this study. Congo Basin domain used in this paper ( $14^{\circ}\text{S}$  to  $4^{\circ}\text{N}$ ,  $18^{\circ}\text{E}$  to  $29^{\circ}\text{E}$ ) is shown by a red box.

instead of direct output from CMIP5, because observed SST in AMIP is prescribed, which removes SST biases that could erroneously impact upon Congo Basin hydrology (Richter et al., 2016). Nevertheless, AMIP runs should be treated with some caution, because fluxes of water and energy from the ocean to the atmosphere are also dependent on the correct specification of the atmosphere (Zhou et al., 2018). Although evaporation data are available across all AMIP models, data for the three components are only available from 17 AMIP models. Some of these models are from the same center, so an ensemble mean of the models might contain biases toward models with similar LSMs. For each center, we therefore retain one AMIP model, selecting the model with the lowest grid spacing. This constrains our analysis to 11 AMIP models.

LSMs embedded within GCMs calculate the three components of evaporation in each grid box in response to meteorological and hydrological inputs, and sum the components to obtain total evaporation (Pitman, 2003). For equations commonly used in GCMs to calculate each evaporation component, see Appendix A. Table 1 also provides details about the equations used to calculate each evaporation component within the LSMs of the 11 AMIP models selected. Data from individual AGCMs are presented in native resolution, and the models are regridded using bilinear interpolation to a common  $1^{\circ} \times 1^{\circ}$  grid before the ensemble mean is calculated. Comparison between models at native and regridded resolution shows that the regridding scheme does not noticeably alter the model output.

### 2.3. Reference Data Sets

In this study, rainfall from each of the 11 AMIP models is compared to the Climate Hazards Group InfraRed Precipitation with Station data v 2.0 (CHIRPS2) (Funk et al., 2015). Evaporation from each of the 11 AMIP models is then compared to LandFlux-EVAL (Mueller et al., 2013). Further details on these data sets are provided in Table 2.

The use of CHIRPS2 in the current study as a reference point is justified for the following two reasons. First, CHIRPS2 has the best agreement of 10 satellite and gauge rainfall products, against a new, gridded, gauge-

**Table 1**  
*AGCMs Used in This Study and Details About Their Evaporation Components*

Model	Grid Spacing	LSM	Canopy Evaporation	Transpiration	Soil Evaporation
bcc-csm1-1-m (Wu et al., 2014)	1.1° × 1.1°	Community Land Model 3 (CLM3) (Oleson et al., 2004) plus AVIM2 Dynamic Vegetation (Ji et al., 2008)	Equation (A1), with additional leaf boundary layer resistance	Equation (A2)	Equation (A3)
BNUEM (Ji et al., 2014)	2.8° × 2.8°	Common Land Model (CoLM) (Dai et al., 2003) plus LPJ Dynamic Vegetation (Sitch et al., 2003)	Equation (A1)	Minimum of atmospheric demand and water supply	Equation (A3)
CanAM4 (Von Salzen et al., 2013)	2.8° × 2.8°	CLASS v2.7 (Verseghy, 2000)	Equation (A1)	Equation (A2)	Equation (A3), with adjustments to account for soil water gradients based on Deardorff equations
CNRM-CM5 (Voldoire et al., 2013)	1.4° × 1.4°	ISBA v3.0 (Decharme & Douville, 2007)	Equation (A1), with subgrid rainfall used in calculating canopy water storage	Equation (A2)	Equation (A3), with humidity at the ground estimated from surface soil moisture
GFDL-HIRAM-C360 (Zhao et al., 2009)	0.3° × 0.3°	LM3.0 (Milly et al., 2014) plus LM3V Dynamic Vegetation (Shevliakova et al., 2009)	Equation (A1)	Equation (A2)	Equation (A3)
GISS-E2-R (Schmidt et al., 2014)	2.5° × 2.0°	GISS 2-LS (Schmidt et al., 2006) plus Ent TBM Dynamic Vegetation (Kim et al., 2015)	Equation (A1), with subgrid rainfall used in calculating canopy water storage	Equation (A2)	Equation (A3)
inmcm4 (Volodin et al., 2010)	2.0° × 1.5°	1-D Model (Volodin & Lykosov, 1998)	Equation (A1), except that an “intercepted rainfall,” equal to half of the rainfall rate, is used in calculating canopy water storage	Equation (A2), except that $F_{dry}$ is a function of soil moisture and soil temperature	Equation (A3), plus Jacquemin and Noilhan (1990) equation to account for soil water gradients
IPSL-CM5A-MR (Dufresne et al., 2013)	2.5° × 1.25°	ORCHIDEE (Krinner et al., 2005)	Equation (A1), with additional leaf boundary layer resistance	Equation (A2)	Minimum of atmospheric demand, and water supply from the top soil layer
MIROC5 (Watanabe et al., 2010)	1.4° × 1.4°	MATSIRO (Takata et al., 2003)	Equation (A1), with rainfall occurring in a fraction of the grid cell for the canopy water storage calculation (no probability distribution)	Equation (A2)	Equation (A3), with adjustments to account for soil water gradients based on a modified surface roughness length
MRI-AGCM3-2S (Mizuta et al., 2012)	0.2° × 0.2°	Hydrology, Atmosphere and Land Model (Hosaka, 2011)	Equation (A1), with additional leaf boundary layer resistance	Equation (A2)	Equation (A3)
NorESM1-M (Bentsen et al., 2013)	2.5° × 1.9°	Community Land Model 4 (CLM4) (Oleson et al., 2010)	Equation (A1), with additional leaf boundary layer resistance	Equation (A2)	Alpha and beta methods (the latter models diffusion of water vapor through the soil)



**Table 2**  
*Reference Data Sets Used in This Study*

Data Set	Grid Spacing	Further Details
CHIRPS v2.0 Rainfall (Funk et al., 2015)	$0.05^\circ \times 0.05^\circ$	High-resolution, quasi-global rainfall data set which merges satellite imagery with in situ station data to produce a gridded rainfall record.
LandFlux-EVAL Evaporation (Mueller et al., 2013)	$1.0^\circ \times 1.0^\circ$	Synthesis product based on a total of 14 remote sensing products, LSMs, reanalyses, diagnostic estimates, and flux tower measurements. All data sets are interpolated onto a common grid before merging.

based rainfall data set (“NIC131-Gridded”) in the Congo Basin (Nicholson et al., 2019). Second, CHIRPS2 has a high spatial resolution of  $0.05^\circ \times 0.05^\circ$ , which enables CHIRPS2 to accurately quantify rainfall delivered to the Congo by mesoscale convective systems (Funk et al., 2015). Conversely, to our knowledge, no evaporation products have been validated in the Congo, because no flux towers are installed (Sjöström et al., 2013), and no trustworthy, long-term ground observations are available for evaporation. However, there are satellite products, evaporation models and synthesis estimates of evaporation, as presented by Trambauer et al. (2014). Unlike rainfall, for which Sylla et al. (2013) show that there is a wide spread between several products in the Congo Basin, Trambauer et al. (2014) show in their Figure 7 that there is excellent consistency among several evaporation products for the magnitude of the annual cycle of evaporation in the Congo Basin. Although the potential exists for a systematic bias across all products, the consistency across multiple products suggests it is more probable than not that the choice of evaporation data set will not substantially affect results. LandFlux-EVAL, a synthesis data set which merges evaporation from a range of LSMs, satellite products and reanalyses, was selected to avoid prioritizing one evaporation algorithm in isolation (Miralles et al., 2016). In addition, the annual cycle from LandFlux-EVAL in the Congo, presented in the current study, compares favorably to the annual cycles presented by Trambauer et al. (2014). Furthermore, LandFlux-EVAL is believed to be a “best guess” estimate of evaporation (Peng et al., 2016), and has been used to evaluate CMIP5 models in previous studies (Mueller & Seneviratne, 2014). The above points strongly support using LandFlux-EVAL as an evaporation reference. To begin our research on model evaporation in an understudied region, the current study uses LandFlux-EVAL as a best guess estimate, notwithstanding the caveat that the lack of validation in the Congo poses. Nevertheless, it may be possible to validate the data set in the near future if flux towers are installed.

## 2.4. Methods

### 2.4.1. Root Mean Square Error Analysis

For each of the 11 models, we first calculate the root mean square error (RMSE) for the annual cycle of rainfall against CHIRPS2, and second calculate the RMSE for the annual cycle of evaporation against LandFlux-EVAL (Table 3). Following the RMSE equation, for each month we calculate the difference between the

model and the reference data and square the result. We then calculate the mean of the 12 months and take the square root to determine the RMSE. After ranking the 11 models from smallest to largest RMSE, a rainfall composite mean is taken across models with rainfall ranks from 1 to 4 (“Realistic Rainfall”), and rainfall ranks from 7 to 11 (“Unrealistic Rainfall”). An evaporation composite mean is then taken across models with rainfall and evaporation ranks from 1 to 4 (“Realistic Evaporation”), and rainfall and evaporation ranks from 7 to 11 (“Unrealistic Evaporation”). The latter is done because models with realistic evaporation must have realistic rainfall. Table 4 lists the models included within each composite.

### 2.4.2. Process-Based Evaluation

In this study we perform a process-based evaluation of the model evaporation, by assessing the credibility of the processes which partition evaporation into its three components. If the models with more realistic evaporation complete this partitioning in a credible way, the three components of evaporation they produce could justifiably provide us with useful information about the character of the annual cycle of total evaporation.

**Table 3**  
*AGCM Rankings for the 30-Year Mean (1979–2008) Annual Cycle of a) Rainfall, and b) Evaporation, in the Congo Basin ( $14^\circ\text{S}$  to  $4^\circ\text{N}$ ,  $18^\circ\text{E}$  to  $29^\circ\text{E}$ )*

Model	Rainfall RMSE	Rainfall Rank	Evaporation RMSE	Evaporation Rank
CNRM-CM5	0.676	1	0.248	1
GFDL-HIRAM-C360	0.787	2	0.776	8
inmcm4	0.863	3	1.237	11
GISS-E2-R	1.014	4	0.460	3
bcc-csm1-1-m	1.035	5	0.525	5
MRI-AGCM3-2S	1.390	6	0.712	7
CanAM4	1.414	7	0.309	2
MIROC5	2.782	8	1.029	9
NorESM1-M	2.901	9	0.612	6
IPSL-CM5A-MR	2.989	10	0.501	4
BNU-ESM	3.375	11	1.052	10

*Note.* CHIRPS2 rainfall (1981–2008) and LandFlux-EVAL evaporation (1989–2005) are used as reference data sets.

**Table 4**  
Models Selected for Each Composite Analyzed Within This Paper

Composite	Unrealistic Rainfall	Realistic Rainfall	Unrealistic Evaporation	Realistic Evaporation
Models Selected	BNU-ESM IPSL-CM5A-MR MIROC5 NorESM1-M	CNRM-CM5 GFDL-HIRAM-C360 GISS-E2-R inmcm4	BNU-ESM MIROC5	CNRM-CM5 GISS-E2-R

In addition, if specific model schemes enable some models to simulate evaporation more realistically for good reasons, it might be possible to argue that these schemes should be used in all models, to improve how models simulate Congo Basin evaporation. The advantage of this might be a narrowing of the model spread in wet season rainfall.

### 3. Annual Cycles of Rainfall and Evaporation in the Congo Basin

Figure 2a shows that the annual cycle of rainfall is bimodal in most models, with two wet seasons and two drier seasons. The model ensemble mean has  $6.35 \text{ mm day}^{-1}$  less rainfall in July, the trough of the summer dry season, than March, the peak of the first wet season. In addition, the ensemble mean has  $0.43 \text{ mm day}^{-1}$  more rainfall in November, the peak of the second wet season, than March, the peak of the first. The largest

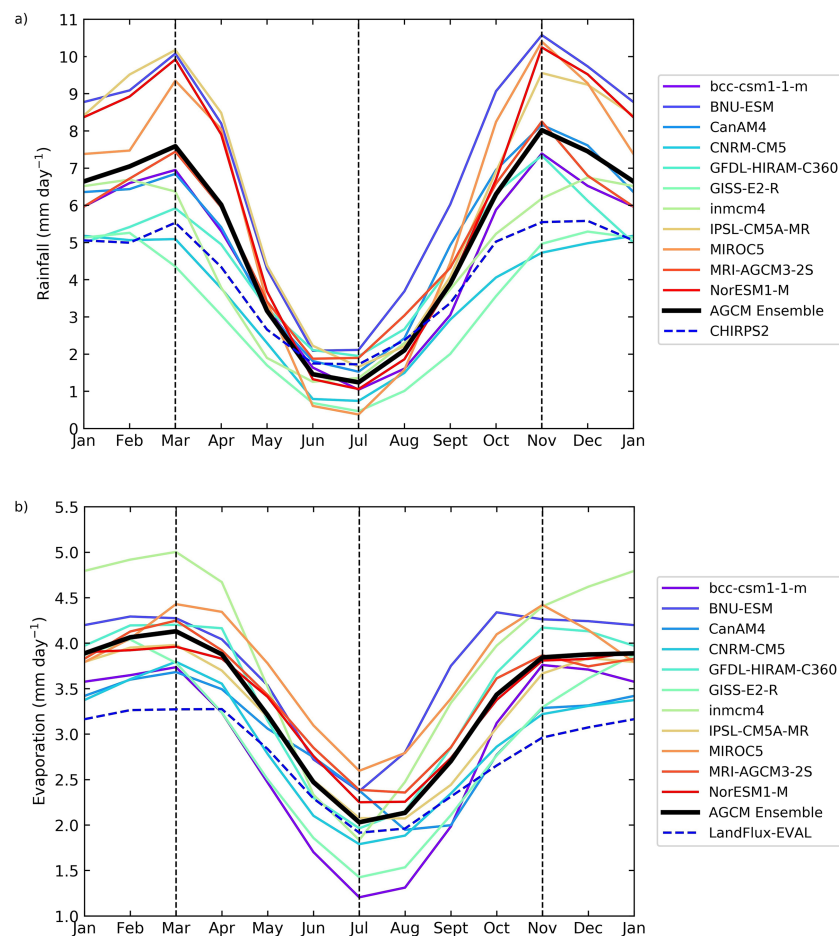


**Figure 2.** Thirty-year mean (1979–2008) annual cycles of rainfall ( $\text{mm day}^{-1}$ ) (a) and evaporation ( $\text{mm day}^{-1}$ ) (b) in the Congo Basin ( $14^{\circ}\text{S}$  to  $4^{\circ}\text{N}$ ,  $18^{\circ}\text{E}$  to  $29^{\circ}\text{E}$ ), from 11 AMIP models, and their ensemble mean. CHIRPS2 rainfall (1981–2008) and LandFlux-EVAL evaporation (1989–2005) are used as reference data sets.

intermodel differences occur in wet months (e.g. March, standard deviation 2.08, and November, standard deviation 2.10), but the smallest intermodel differences occur in drier months (e.g. July, standard deviation 0.60). It is also interesting to note that most models overestimate CHIRPS2 rainfall in the two wet seasons, but not in the summer dry season. Conversely, Figure 2b shows that the annual cycle of evaporation in most models has a decline in evaporation between March and July, but recovery between July and November. The model ensemble mean has  $2.10 \text{ mm day}^{-1}$  less evaporation in July than March and  $0.29 \text{ mm day}^{-1}$  less evaporation in November than March. In contrast to rainfall, the spread in evaporation between models is very small throughout the annual cycle. For example, standard deviations are 0.39 in March, 0.43 in July, and 0.44 in November. Nevertheless, Figure 2b also shows that the majority of models overestimate LandFlux-EVAL evaporation in the two wet seasons, but not in the summer dry season.

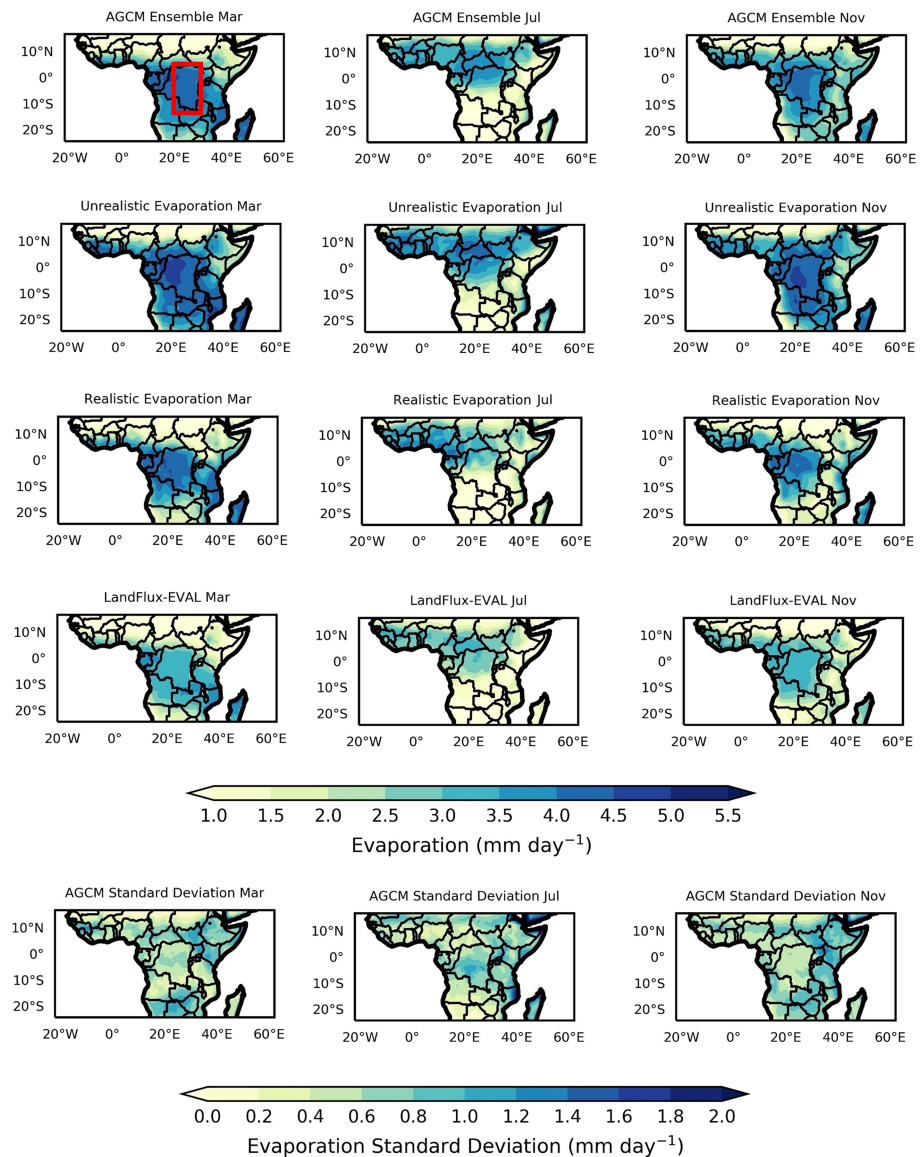
Table 3 describes the RMSE ranking of the individual models for both rainfall and evaporation (see section 2 for a description of the methodology). CNRM-CM5 and GISS-E2-R have small errors for both rainfall and evaporation, while BNU-ESM and MIROC5 have large errors for both rainfall and evaporation. However, models with small errors for rainfall do not always have small errors for evaporation, and vice versa. For example, GFDL-HIRAM-C360 and Inmcm4 have small errors for rainfall, but large errors for evaporation. This could be because these two models have errors in their land surface schemes which convert rainfall to evaporation, or because they have errors in other important variables which are required to produce evaporation, such as solar radiation. Conversely, CanAM4 and IPSL-CM5A-MR have large errors for rainfall but small errors for evaporation. As these two models have too much rainfall, interception and reevaporation from the canopy might be too large. The effect would be to suppress transpiration from plant stomata, as the atmospheric demand for evaporation would be erroneously satisfied (Lawrence et al., 2007). These two models might produce a realistic amount of evaporation, but for the incorrect reason, because their ratio of canopy evaporation to transpiration could be incorrect (Wang & Eltahir, 2000).

Figure 3 shows the spatial distribution of evaporation at the turning points of the evaporation annual cycle. In March, the band of peak evaporation in the model ensemble mean is in the center of the basin. Evaporation rates are highest in the composite of models with “unrealistic” evaporation, lower in the composite of models with “realistic” evaporation, and lower still in LandFlux-EVAL. By July, the band of peak evaporation has migrated to the north in the model ensemble mean. This band is strong in models with unrealistic evaporation, not as strong in models with realistic evaporation, and in between these two in LandFlux-EVAL. By November, the band of peak evaporation in the model ensemble mean has migrated back southward. Once more, evaporation rates are highest in models with unrealistic evaporation, lower in models with realistic evaporation, and even lower still in LandFlux-EVAL. AGCM standard deviations are small throughout the year.

Figure 4a shows that rainfall is  $3.81 \text{ mm day}^{-1}$  lower in March,  $0.04 \text{ mm day}^{-1}$  lower in July and  $3.78 \text{ mm day}^{-1}$  lower in November in models with realistic rainfall compared to unrealistic rainfall. The reduction in rainfall during the wet seasons causes greater coherence between the annual cycle of rainfall in the models and CHIRPS2, with an RMSE of 0.56 for models with realistic rainfall as compared to 2.99 for models with unrealistic rainfall. Models with realistic rainfall also simulate less rainfall in July than March ( $-4.97 \text{ mm day}^{-1}$ ), and more rainfall in November than March ( $+0.29 \text{ mm day}^{-1}$ ). The latter is consistent with Jackson et al. (2009), who argued that the presence of the southern component of the African Easterly Jet in boreal autumn increases the frequency of mesoscale convective systems in the second wet season, which increases rainfall.

Conversely, Figure 4b shows that evaporation is  $0.45 \text{ mm day}^{-1}$  lower in March,  $0.84 \text{ mm day}^{-1}$  lower in July and  $0.97 \text{ mm day}^{-1}$  lower in November in models with realistic evaporation compared to models with unrealistic evaporation. This causes greater coherence between the annual cycle of evaporation in models and LandFlux-EVAL, with an RMSE of 0.38 for models with realistic evaporation as compared to 1.01 for models with unrealistic evaporation. In addition, models with realistic evaporation simulate less evaporation in July than March ( $-2.23 \text{ mm day}^{-1}$ ), and importantly, less evaporation in November than March ( $-0.55 \text{ mm day}^{-1}$ ).

The above analysis highlights two important characteristics about the annual cycle of evaporation in the Congo Basin. First, the realistic models and reference data show that evaporation is lower in the summer dry season than the first wet season. Second, the realistic models and reference data show that



**Figure 3.** Thirty-year mean (1979–2008) evaporation (mm day<sup>-1</sup>) for March, July, and November, from the AGCM ensemble mean, models with unrealistic evaporation, models with realistic evaporation, and LandFlux-EVAL. AGCM standard deviations are also included. Domain analyzed in this paper (14°S to 4°N, 18°E to 29°E) is shown by a red box in the first panel.

evaporation is lower in the second wet season than the first, despite higher rainfall in the second. Both of these characteristics are, to our knowledge, not understood. The former is consistent with a plausible positive feedback (Seneviratne et al., 2010), whereby lower rainfall during the summer dry season would result in lower soil moisture, which would reduce evaporation. However, the latter is not consistent with a positive feedback. Instead, higher rainfall in November corresponds with lower evaporation in November. The latter suggests that the two wet seasons have very different climatological and hydrological characteristics, which are worthy of exploration.

An analysis to attribute what is causing lower evaporation in November than March would require splitting the Congo into the northern rainforest and southern savannah, and is beyond the scope of this study. However, it might still be possible to obtain some useful information about this feature from the evaporation partitioning, to aid a future attribution. In the next section, we focus our process-based evaluation on the two wet seasons. We examine the credibility of the processes which partition evaporation into its three components in the models with realistic evaporation in March and November. If the processes are credible, we will

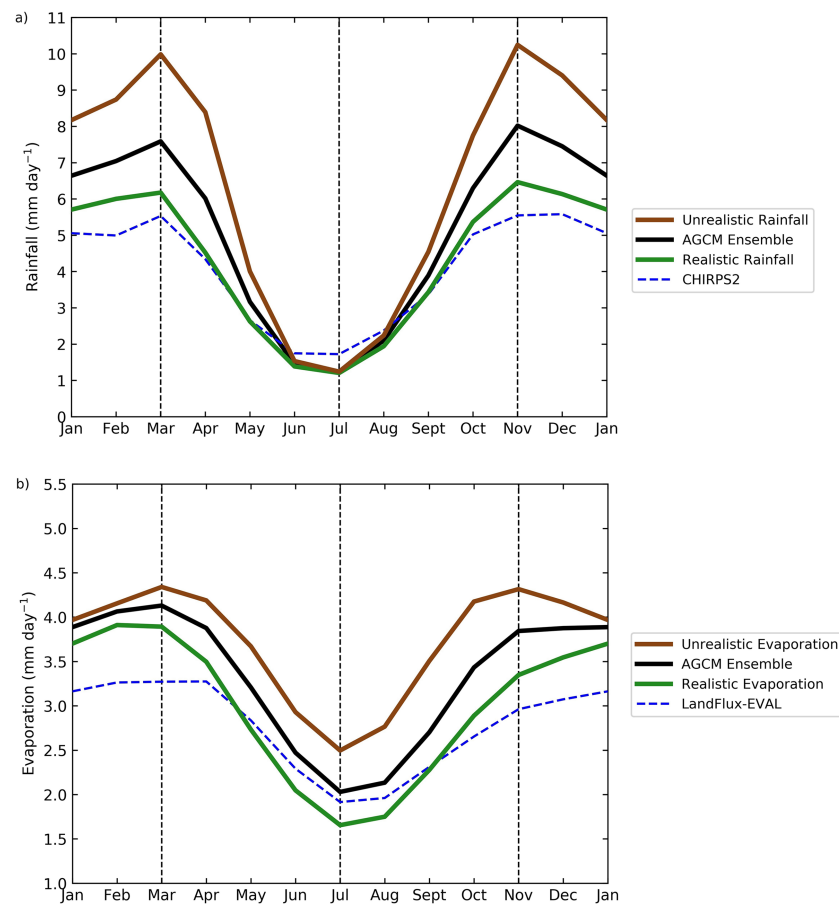


**Figure 4.** Thirty-year mean (1979–2008) annual cycles of rainfall ( $\text{mm day}^{-1}$ ) (a) and evaporation ( $\text{mm day}^{-1}$ ) (b) in the Congo Basin ( $14^{\circ}\text{S}$  to  $4^{\circ}\text{N}$ ,  $18^{\circ}\text{E}$  to  $29^{\circ}\text{E}$ ). Rainfall annual cycles are from models with unrealistic rainfall, the AGCM ensemble mean, and models with realistic rainfall. Evaporation annual cycles are from models with unrealistic evaporation, the AGCM ensemble mean, and models with realistic evaporation. CHIRPS2 rainfall and LandFlux-EVAL evaporation are used as reference data sets.

be able to obtain information from the evaporation partitioning regarding the negative evaporation difference between March and November. In addition, we might be able to suggest whether certain schemes should be used in more models to improve evaporation during the wet seasons specifically. As the Congo Basin is believed to be a hot spot of moisture recycling during the wet seasons (Dyer et al., 2017), this might help to constrain the model spread in rainfall evident during the two wet seasons.

## 4. Evaporation Partitioning in the Congo Basin Wet Seasons

### 4.1. Canopy Evaporation

Table 1 shows that models with realistic evaporation (CNRM-CM5 and GISS-E2-R) use subgrid rainfall schemes in their land surface components. These approaches follow Eltahir and Bras (1993) to correct the “GCM drizzle” problem, whereby intense convective rainfall at scales below the grid box can only be represented as grid box average rainfall of lower intensity. Subgrid rainfall schemes modify the fractional coverage of rainfall in each grid box, and distribute rainfall intensity according to a probability density function. Physically, the action of these schemes is to increase canopy throughfall, reduce canopy water storage, and reduce canopy evaporation. Conversely, models with unrealistic evaporation (BNU-ESM and MIROC5) do not use subgrid rainfall schemes. As a result, the canopy is more easily able to intercept the low intensity rainfall, and the models simulate low canopy throughfall, high canopy water storage, and high canopy evaporation. Subgrid rainfall schemes offer an explanation for why canopy evaporation is  $1.12 \text{ mm day}^{-1}$  lower in March and  $1.10 \text{ mm day}^{-1}$  lower in November in models with realistic evaporation than in models with



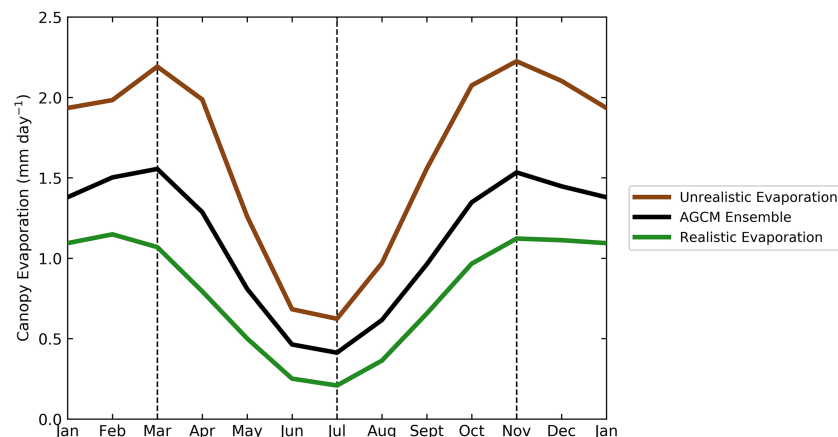


**Figure 5.** Thirty-year mean (1979–2008) annual cycle of canopy evaporation ( $\text{mm day}^{-1}$ ) in the Congo Basin ( $14^{\circ}\text{S}$  to  $4^{\circ}\text{N}$ ,  $18^{\circ}\text{E}$  to  $29^{\circ}\text{E}$ ) from models with unrealistic total evaporation, the AGCM ensemble mean, and models with realistic total evaporation.

unrealistic evaporation, as shown in Figure 5. Nevertheless, canopy evaporation in models with realistic evaporation occurs at a similar rate in both March and November.

#### 4.2. Transpiration

Figure 6 shows that transpiration is  $0.85 \text{ mm day}^{-1}$  higher in March and  $0.32 \text{ mm day}^{-1}$  higher in November in models with realistic evaporation than in models with unrealistic evaporation. As the models with realistic evaporation contain subgrid rainfall schemes, canopy evaporation is decreased in these models relative to models with unrealistic evaporation. This means that the atmospheric demand for evaporation is not satisfied, so transpiration increases in March and November (Lawrence et al., 2007). However, the increase in transpiration is less than the decrease in canopy evaporation, because transpiration is typically calculated with reference to canopy resistance terms (Equation A2). As a result, total evaporation is realistically brought down into better agreement with LandFlux-EVAL, as shown by Figure 4b. In addition, the ratio of transpiration to total evaporation increases during the wet seasons, and these models are credibly brought into agreement with studies which suggest that transpiration in the Congo should be a larger component of evaporation than most models simulate (Lian et al., 2018). Subgrid rainfall schemes therefore cause the models to simulate evaporation in a realistic manner in the wet seasons, by credibly adjusting down the fraction of canopy evaporation and adjusting up the fraction of transpiration. However, Figure 6 also shows that when the

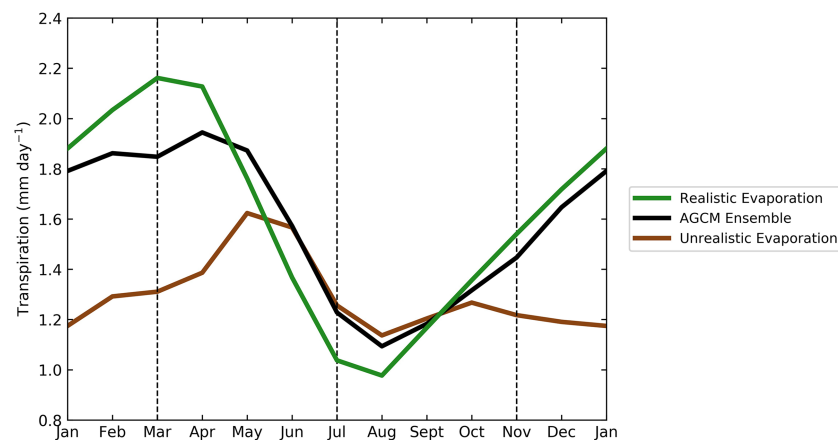


**Figure 6.** Thirty-year mean (1979–2008) annual cycle of transpiration ( $\text{mm day}^{-1}$ ) in the Congo Basin ( $14^{\circ}\text{S}$  to  $4^{\circ}\text{N}$ ,  $18^{\circ}\text{E}$  to  $29^{\circ}\text{E}$ ) from models with realistic total evaporation, the AGCM ensemble mean, and models with unrealistic total evaporation.

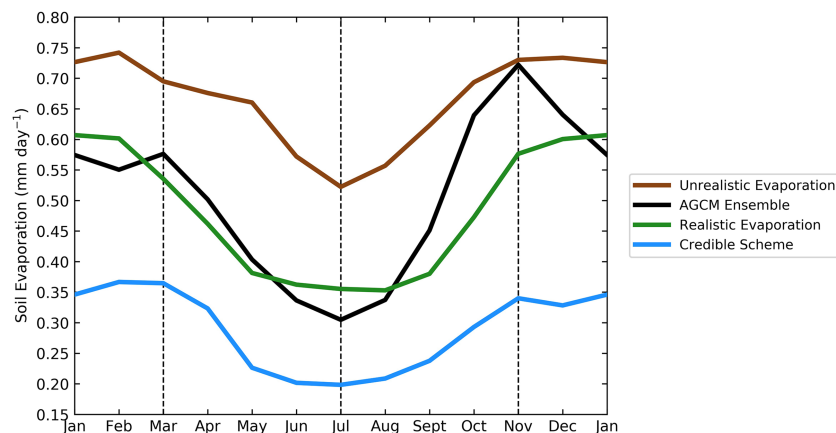


**Figure 7.** Thirty-year mean (1979–2008) annual cycle of soil evaporation ( $\text{mm day}^{-1}$ ) in the Congo Basin ( $14^{\circ}\text{S}$  to  $4^{\circ}\text{N}$ ,  $18^{\circ}\text{E}$  to  $29^{\circ}\text{E}$ ) from models with unrealistic total evaporation, the AGCM ensemble mean, models with realistic total evaporation, and models which contain a credible scheme for soil evaporation (refer to section 4.3).

fraction of transpiration is high in models with realistic evaporation, transpiration is suppressed by  $0.62 \text{ mm day}^{-1}$  in November relative to March. To date, it is unclear why, at a time when there is more rainfall in the Congo, models with realistic evaporation suggest that less transpiration is released from the vegetation.

#### 4.3. Soil Evaporation

Figure 7 shows that soil evaporation is  $0.16 \text{ mm day}^{-1}$  lower in March and  $0.15 \text{ mm day}^{-1}$  lower in November in models with realistic evaporation as compared to models with unrealistic evaporation. Soil evaporation in models with realistic evaporation is therefore a small fraction of the total evaporation in the wet seasons. In addition, soil evaporation in models with realistic evaporation occurs at a similar rate in both March and November. However, the above characteristics of soil evaporation are not believable improvements. This is because there is no credible reason which explains why soil evaporation is lower in the models with realistic evaporation compared to others.

Nevertheless, four models from the set of 11 (as detailed in Table 1) include a scheme which plausibly decreases specific humidity in the top soil layer to account for soil water gradients (Jacquemin & Noilhan, 1990). This scheme is not considered by any of the other models, and is distributed across models, rather than being solely associated with models that have realistic evaporation. Figure 7 shows that in a composite of the models with this credible scheme for soil evaporation (CanAM4, CNRM-CM5, Inmcm4 and MIROC5), the models have  $0.21$  and  $0.38 \text{ mm day}^{-1}$  less soil evaporation in March and November respectively than the model ensemble mean. In addition, the difference in soil evaporation between March and November is  $-0.02 \text{ mm day}^{-1}$ . This allows us to argue with more confidence that soil evaporation might be lower in reality than most models suggest, and is not likely to differ substantially between March and November.

### 5. Discussion

Models with realistic evaporation include subgrid rainfall schemes in their land surface components. During wet seasons, these schemes credibly decrease canopy evaporation, which causes increased transpiration to satisfy the atmospheric demand for evaporation. The upward adjustment in transpiration is plausible, as the transpiration is brought into agreement with studies which suggest that there is a high ratio of transpiration to total evaporation in the Congo Basin (Wei et al., 2017). In addition, the downward adjustment in canopy evaporation is greater than the upward increase in transpiration in both March and November, because canopy resistance terms cap the increase in transpiration. This reduces total evaporation in both March and November to more realistic values, which are comparable with LandFlux-EVAL (Figure 4b), and suggests that models with more realistic evaporation, that have subgrid rainfall schemes, are producing evaporation in a more credible and realistic manner during the wet seasons.

Table 5 shows that in models with unrealistic evaporation, the differences in the three evaporation components between March and November are very small. This explains why evaporation does not notably change

**Table 5**

Thirty-Year Mean (1979–2008) Difference in Total Evaporation and Its Three Components Between March and November, From Model Composites with a) Unrealistic Evaporation, and b) Realistic Evaporation. Values Are Averaged Over The Congo Basin (14°S to 4°N, 18°E to 29°E)

	$\Delta$ Total Evaporation	$\Delta$ Canopy Evaporation	$\Delta$ Transpiration	$\Delta$ Soil Evaporation
Difference between March and November (Unrealistic Evaporation)	−0.02	+0.03	−0.10	+0.04
Difference between March and November (Realistic Evaporation)	−0.55	+0.05	−0.62	+0.04

Note. Units are  $\text{mm day}^{-1}$ .

in these models between March and November ( $-0.02 \text{ mm day}^{-1}$ ). Table 5 also shows that in models with realistic evaporation, the climatological difference between March and November is  $-0.62 \text{ mm day}^{-1}$  for transpiration,  $+0.05 \text{ mm day}^{-1}$  for canopy evaporation, and  $+0.04 \text{ mm day}^{-1}$  for soil evaporation. Therefore, importantly, Table 5 shows that the suppression of the transpiration component in November relative to March is almost fully responsible for the  $0.55 \text{ mm day}^{-1}$  lower evaporation in November than March in these models.

In models with subgrid rainfall, because total evaporation is more realistic, and because transpiration and canopy evaporation are more realistically partitioned, we argue that the lower transpiration in November than March, and similar canopy evaporation in November and March, are likely to be trustworthy differences. In addition, a composite of models containing a credible scheme for soil evaporation shows no substantial difference in soil evaporation between November and March (Figure 7), which suggests that a negligible difference in soil evaporation is also likely to be trustworthy. We therefore argue that climatologically, lower transpiration is likely to explain why evaporation is lower in November than March in reality. However, as stated in section 4, it is not clear why, when there is more rainfall in the Congo Basin in November, models with realistic evaporation suggest that there is less transpiration from the vegetation. Further research is therefore needed to investigate what factors might be responsible.

As subgrid rainfall schemes enable models to simulate evaporation with increased realism during the wet seasons, by making plausible adjustments to the ratio of transpiration to canopy evaporation, we suggest that using subgrid rainfall schemes in the land surface components of all GCMs could improve how models produce evaporation from the Congo Basin during the wet seasons. This might also have benefits for how models simulate the wider hydrological cycle of the region. Creese et al. (2019) suggested that improving how models represent the two African Easterly Jets could reduce the model spread in Congo Basin wet season rainfall. Additionally, given that the Congo is a potential hot spot of moisture recycling, it is possible that using subgrid rainfall schemes in all GCMs to improve how models represent Congo Basin evaporation during both wet seasons could further reduce the model spread in wet season rainfall.

## 6. Conclusions

In this study, we performed a process-based evaluation of the evaporation climatology for the Congo Basin wet seasons in 11 CMIP5 models contributing to AMIP. The key findings are as follows:

1. GCMs with realistic rainfall in the Congo simulate higher rainfall in November, the peak of the second wet season, than March, the peak of the first, on the climatological average.
2. GCMs with realistic evaporation in the Congo simulate lower evaporation in November than March, because these models suppress transpiration.
3. In both wet seasons, subgrid rainfall schemes in the GCMs with realistic evaporation make the models simulate a credible ratio of transpiration to canopy evaporation, and cause them to bring evaporation down into better agreement with LandFlux-EVAL reference data.
4. As a result, we broadly trust how evaporation is produced in the two wet seasons in the models with realistic evaporation, and argue that lower transpiration is likely to explain why evaporation is lower in November than March in reality.
5. In addition, we suggest that using subgrid rainfall schemes in the land surface components of all GCMs could improve how the models produce Congo Basin evaporation during both wet seasons.

It is unclear why there would be less transpiration in November than March across the Congo Basin, when more rainfall is delivered to the Congo Basin in November. The processes controlling the lower November

transpiration are likely to be crucial in explaining why the annual cycle of evaporation on the domain-wide average varies as it does. A follow-up attribution analysis, in preparation by the authors, therefore aims to investigate what factors might be responsible. In addition, it is still unclear why models and reference data have lower evaporation in the summer dry season than the first wet season, and the authors are considering researching this in future.

As the Congo Basin is believed to be a hot spot of moisture recycling, using subgrid rainfall schemes to improve how models produce Congo evaporation could lead to improvements in how models generate Congo rainfall. If implemented across models, this might lead to a narrowing of the large model spread in wet season rainfall in the Congo Basin. Further research is needed to confirm this hypothesis, and to examine whether using subgrid rainfall schemes might provide hydrological benefits for other regions too. If the benefits are widespread, then consideration should be given to including these schemes as standard in the next generation of GCMs (Pitman, 1991).

## Appendix A: Evaporation Partitioning in LSMs

### A1. Canopy Evaporation

LSMs typically incorporate an equation which considers a balance between rainfall, canopy evaporation, and canopy throughfall in the previous time step to predict canopy water storage. LSMs then use leaf area index (the one-sided leaf area per unit ground area), which is either prescribed from satellite data (e.g., Running et al., 2017), or predicted using a dynamic vegetation model (Yu et al., 2016), to calculate the fraction of wet foliage. This is then typically used to scale potential evaporation, or the amount of evaporation that would occur if the water supply were sufficient, to an estimate of the current evaporation of water from the canopy store, as follows:

$$E_c = F_{\text{wet}} \rho \frac{qsat(T_s) - q_a}{r_a} \quad (\text{A1})$$

where  $F_{\text{wet}}$  is the fraction of wet foliage,  $\rho$  is the density of air,  $qsat(T_s)$  is the saturation specific humidity at near-surface air temperature  $T_s$ ,  $q_a$  is the atmospheric specific humidity, and  $r_a$  is an aerodynamic resistance, which depends on a drag coefficient and on wind speed.

### A2. Transpiration

To calculate transpiration (or the flux of water vapor from plant stomata into the atmosphere), LSMs typically scale potential evaporation by the fraction of dry foliage, as follows:

$$E_t = F_{\text{dry}} \rho \frac{qsat(T_s) - q_a}{r_a + r_c} \quad (\text{A2})$$

where the equation uses  $F_{\text{dry}}$  (the fraction of dry foliage, equal to  $1 - F_{\text{wet}}$ ), and an additional term  $r_c$ , the canopy resistance to transpiration. This defines the balance between the desire to close stomata to minimize transpiration, and open stomata to take in  $\text{CO}_2$  (the “stomatal conductance”), scaled up to the canopy leaf area (Damour et al., 2010). The canopy leaf area controls the number of stomata, and sets upper limits on plant transpiration (Jarvis & McNaughton, 1986).

### A3. Soil Evaporation

“Alpha” methods are typically used to calculate soil evaporation in LSMs. An equation for the alpha method is of the following form (Mahfouf et al., 1995):

$$E_s = \rho \frac{\alpha qsat(T_g) - q_a}{r_a} \quad (\text{A3})$$

where  $qsat(T_g)$  is the saturation specific humidity at ground surface temperature  $T_g$ , and alpha is a coefficient which scales down this humidity to an estimate of the actual specific humidity of the upper soil layer. Note that  $T_g$  is used rather than  $T_s$ , because this allows for shortwave radiation to control the soil evaporation. In forest regions, a high leaf area reduces shortwave radiation penetrating to the ground surface, reduces  $T_g$ , and reduces soil evaporation (Wang & Liu, 2007). In many LSMs, alpha is defined by the

thermodynamic relationship of Philip (1957), which depends on the soil matrix potential. This defines the maximum amount of water that can be retained in the soil and is typically related to properties such as soil pore size (Whalley et al., 2013).

## Acknowledgments

David Crowhurst is supported by the U.K. Natural Environment Research Council (NERC) through the DTP in Environmental Research (Grant NE/L002612/1). Richard Washington is supported by the NERC-Department for International Development (DFID)-funded Improving Model Processes for African Climate (IMPALA) project (Grant NE/M017206/1), as part of the Future Climate for Africa (FCFA) project (<http://www.futureclimateafrica.org/project/impala/>). AGCM data used in this study were downloaded from the Earth System Grid Federation (ESGF) (at <https://pcmdi.llnl.gov/>). CHIRPS2 data were downloaded from the Climate Hazards Group ([ftp://ftp.chg.ucsb.edu/pub/org/chg/products/CHIRPS-2.0/global\\_monthly/netcdf/](ftp://ftp.chg.ucsb.edu/pub/org/chg/products/CHIRPS-2.0/global_monthly/netcdf/), accessed 21 January 2020). This study uses the LandFlux-EVAL merged benchmark synthesis products of ETH Zurich produced under the aegis of the GEWEX and ILEAPS projects (<http://www.iac.ethz.ch/url/research/LandFlux-EVAL/>). The authors acknowledge the helpful inputs of Amy Creese, Ellen Dyer, and Jian Peng in preparing the manuscript. We also thank the Editor and one anonymous reviewer, whose comments helped us to considerably improve the quality of the manuscript.

## References

- Bele et al. (2015). Adapting the Congo Basin forests management to climate change: Linkages among biodiversity, forest loss, and human well-being. *Forest Policy and Economics*, 50, 1–10. <https://doi.org/10.1016/J.FORPOL.2014.05.010>
- Bentsen, M., Bethke, I., Debernard, J. B., Iversen, T., Kirkevåg, A., Seland, Ø., et al. (2013). The Norwegian Earth System Model, NorESM1-M—Part 1: Description and basic evaluation of the physical climate. *Geoscientific Model Development*, 6(3), 687–720. <https://doi.org/10.5194/gmd-6-687-2013>
- Creese, A., & Washington, R. (2016). Using qflux to constrain modeled Congo Basin rainfall in the CMIP5 ensemble. *Journal of Geophysical Research: Atmospheres*, 121, 13,415–13,442. <https://doi.org/10.1002/2015JD024524>
- Creese, A., & Washington, R. (2018). A process-based assessment of CMIP5 rainfall in the Congo Basin: The September–November rainy season. *Journal of Climate*, 31, 7417–7439. <https://doi.org/10.1175/JCLI-D-17-0818.1>
- Creese, A., Washington, R., & Munday, C. (2019). The plausibility of September–October–November Congo Basin rainfall change in coupled climate models. *Journal of Geophysical Research: Atmospheres*, 124, 5822–5846. <https://doi.org/10.1029/2018JD029847>
- Dai, Y., Zeng, X., Dickinson, R. E., Baker, I., Bonan, G. B., Bosilovich, M. G., et al. (2003). The common land model. *Bulletin of the American Meteorological Society*, 84(8), 1013–1024. <https://doi.org/10.1175/BAMS-84-8-1013>
- Damour, G., Simonneau, T., Cochard, H., & Urban, L. (2010). An overview of models of stomatal conductance at the leaf level. *Plant, Cell and Environment*, 33, 1419–1438. <https://doi.org/10.1111/j.1365-3040.2010.02181.x>
- Dargie, G. C., Lawson, I. T., Rayden, T. J., Miles, L., Mitchard, E. T. A., Page, S. E., et al. (2018). Congo Basin peatlands: Threats and conservation priorities. *Mitigation and Adaptation Strategies for Global Change*, 24(4), 669–686. <https://doi.org/10.1007/s11027-017-9774-8>
- Dargie, G. C., Lewis, S. L., Lawson, I. T., Mitchard, E. T. A., Page, S. E., Bocko, Y. E., & Ifo, S. A. (2017). Age, extent and carbon storage of the central Congo Basin peatland complex. *Nature*, 542(7639), 86–90. <https://doi.org/10.1038/nature21048>
- Decharme, B., & Douville, A. H. (2007). Global validation of the ISBA sub-grid hydrology. *Climate Dynamics*, 29(1), 21–37. <https://doi.org/10.1007/s00382-006-0216-7>
- Dufresne, J. L., Foujols, M. A., Denvil, S., Caubel, A., Marti, O., Aumont, O., et al. (2013). Climate change projections using the IPSL-CM5 Earth System Model: from CMIP3 to CMIP5. *Climate Dynamics*, 40(9–10), 2123–2165. <https://doi.org/10.1007/s00382-012-1636-1>
- Dyer, E. L. E., Jones, D. B. A., Nausbaumer, J., Li, H., Collins, O., Vettoretti, G., & Noone, D. (2017). Congo Basin precipitation: Assessing seasonality, regional interactions, and sources of moisture. *Journal of Geophysical Research: Atmospheres*, 122(13), 6882–6898. <https://doi.org/10.1002/2016JD026240>
- Eltahir, E. A. B., & Bras, R. L. (1993). A description of rainfall interception over large areas. *Journal of Climate*, 6(6), 1002–1008. [https://doi.org/10.1175/1520-0442\(1993\)006<1002:ADORIO>2.0.CO;2](https://doi.org/10.1175/1520-0442(1993)006<1002:ADORIO>2.0.CO;2)
- Funk, C., Peterson, P., Landsfeld, M., Pedreros, D., Verdin, J., Shukla, S., et al. (2015). The climate hazards infrared precipitation with stations—A new environmental record for monitoring extremes. *Scientific Data*, 2, 150066. <https://doi.org/10.1038/sdata.2015.66>
- Haensler, A., Saeed, F., & Jacob, D. (2013). Assessing the robustness of projected precipitation changes over central Africa on the basis of a multitude of global and regional climate projections. *Climatic Change*, 121(2), 349–363. <https://doi.org/10.1007/s10584-013-0863-8>
- Hosaka, M. (2011). A new MRI land surface model HAL. *AGU Fall Meeting Abstracts*.
- Jackson, B., Nicholson, S. E., & Klotter, D. (2009). Mesoscale convective systems over western equatorial Africa and their relationship to large-scale circulation. *Monthly Weather Review*, 137(4), 1272–1294. <https://doi.org/10.1175/2008MWR2525.1>
- Jacquemin, B., & Noilhan, J. (1990). Sensitivity study and validation of a land surface parameterization using the HAPEX-MOBILHY data set. *Boundary-Layer Meteorology*, 52(1–2), 93–134. <https://doi.org/10.1007/BF00123180>
- James, R., Washington, R., Abiodun, B., Kay, G., Mutemi, J., Pokam, W., et al. (2018). Evaluating climate models with an African lens. *Bulletin of the American Meteorological Society*, 99(2), 313–336. <https://doi.org/10.1175/BAMS-D-16-0090.1>
- Jarvis, P. G., & McNaughton, K. G. (1986). Stomatal control of transpiration: Scaling up from leaf to region. *Advances in Ecological Research*, 15, 1–49. [https://doi.org/10.1016/S0065-2504\(08\)60119-1](https://doi.org/10.1016/S0065-2504(08)60119-1)
- Ji, D., Wang, L., Feng, J., Wu, Q., Cheng, H., Zhang, Q., et al. (2014). Description and basic evaluation of Beijing Normal University Earth System Model (BNU-ESM) version 1. *Geoscientific Model Development*, 7(5), 2039–2064. <https://doi.org/10.5194/gmd-7-2039-2014>
- Ji, J. J., Huang, M., & Li, K. R. (2008). Prediction of carbon exchanges between China terrestrial ecosystem and atmosphere in 21st century. *Science in China, Series D: Earth Sciences*, 51(6), 885–898. <https://doi.org/10.1007/s11430-008-0039-y>
- Jury, M. R., & Mpetia, E. J. (2009). African climate variability in the satellite era. *Theoretical and Applied Climatology*, 98(3–4), 279–291. <https://doi.org/10.1007/s00704-009-0106-0>
- Kim, Y., Moorcroft, P. R., Aleinov, I., Puma, M. J., & Kiang, N. Y. (2015). Variability of phenology and fluxes of water and carbon with observed and simulated soil moisture in the Ent Terrestrial Biosphere Model (Ent TBM version 1.0.1.0.0). *Geoscientific Model Development*, 8(12), 3837–3865. <https://doi.org/10.5194/gmd-8-3837-2015>
- Krinner, G., Viovy, N., de Noblet-Ducoudré, N., Ogée, J., Polcher, J., Friedlingstein, P., et al. (2005). A dynamic global vegetation model for studies of the coupled atmosphere-biosphere system. *Global Biogeochemical Cycles*, 19, GB1015. <https://doi.org/10.1029/2003GB002199>
- Lawrence, D. M., Thornton, P. E., Oleson, K. W., & Bonan, G. B. (2007). The partitioning of evapotranspiration into transpiration, soil evaporation, and canopy evaporation in a GCM: Impacts on land–atmosphere interaction. *Journal of Hydrometeorology*, 8(4), 862–880. <https://doi.org/10.1175/JHM596.1>
- Lian, X., Piao, S., Huntingford, C., Li, Y., Zeng, Z., Wang, X., et al. (2018). Partitioning global land evapotranspiration using CMIP5 models constrained by observations. *Nature Climate Change*, 8(7), 640–646. <https://doi.org/10.1038/s41558-018-0207-9>
- Mahfouf, J. F., Manzi, A. O., Noilhan, J., Giordani, H., & Deque, M. (1995). The land surface scheme ISBA within the Mete-France climate model ARPEGE. Part I: Implementation and preliminary results. *Journal of Climate*, 8(8), 2039–2057. [https://doi.org/10.1175/1520-0442\(1995\)008<2039:TLSSIW>2.0.CO;2](https://doi.org/10.1175/1520-0442(1995)008<2039:TLSSIW>2.0.CO;2)



- Milly, P. C. D., Malyshev, S. L., Shevliakova, E., Dunne, K. A., Findell, K. L., Gleeson, T., et al. (2014). An enhanced model of land water and energy for global hydrologic and Earth-system studies. *Journal of Hydrometeorology*, 15(5), 1739–1761. <https://doi.org/10.1175/JHM-D-13-0162.1>
- Miralles, D. G., Jiménez, C., Jung, M., Michel, D., Ershadi, A., McCabe, M. F., et al. (2016). The WACMOS-ET project—Part 2: Evaluation of global terrestrial evaporation data sets. *Hydrology and Earth System Sciences*, 20(2), 823–842. <https://doi.org/10.5194/hess-20-823-2016>
- Mizuta, R., Yoshimura, H., Murakami, H., Matsudea, M., Endo, H., Tomoaki, O., et al. (2012). Climate simulations using MRI-AGCM3.2 with 20-km grid. *Journal of the Meteorological Society of Japan*, 90A, 233–258. <https://doi.org/10.2151/jmsj.2012-A12>
- Mueller, B., Hirschi, M., Jimenez, C., Ciais, P., Dirmeyer, P. A., Dolman, A. J., et al. (2013). Benchmark products for land evapotranspiration: LandFlux-EVAL multi-data set synthesis. *Hydrology and Earth System Sciences*, 17(10), 3707–3720. <https://doi.org/10.5194/hess-17-3707-2013>
- Mueller, B., & Seneviratne, S. I. (2014). Systematic land climate and evapotranspiration biases in CMIP5 simulations. *Geophysical Research Letters*, 41(1), 128–134. <https://doi.org/10.1002/2013GL058055>
- Nicholson, S. E., Klotter, D., Zhou, L., & Hua, W. (2019). Validation of satellite precipitation estimates over the Congo Basin. *Journal of Hydrometeorology*, 20(4), 631–656. <https://doi.org/10.1175/JHM-D-18-0118.1>
- Oleson, K., Dai, Y., Bonan, B., Bosilovich, M., Dickinson, R., Dirmeyer, P., et al. (2004). Technical description of the Community Land Model (CLM). <https://doi.org/10.5065/D6N877R0>
- Oleson, W., Lawrence, M., Bonan, B., Flanner, G., Kluzek, E., Lawrence, J., et al. (2010). Technical description of version 4.0 of the Community Land Model (CLM). <https://doi.org/10.5065/D6FB50WZ>
- Peng, J., Loew, A., Chen, X., Ma, Y., & Su, Z. (2016). Comparison of satellite-based evapotranspiration estimates over the Tibetan Plateau. *Hydrology and Earth System Sciences*, 20(8), 3167–3182. <https://doi.org/10.5194/hess-20-3167-2016>
- Philip, J. R. (1957). Evaporation, and moisture and heat fields in the soil. *Journal of Meteorology*, 14. [https://doi.org/10.1175/1520-0469\(1957\)014<0354:EAMAHF>2.0.CO;2](https://doi.org/10.1175/1520-0469(1957)014<0354:EAMAHF>2.0.CO;2)
- Pitman, A. J. (1991). Sensitivity of the land surface to sub-grid scale processes: Implications for climate simulations. *Plant Ecology*, 91(1–2), 121–134. <https://doi.org/10.1007/BF00036052>
- Pitman, A. J. (2003). The evolution of, and revolution in, land surface schemes designed for climate models. *International Journal of Climatology*, 23(5), 479–510. <https://doi.org/10.1002/joc.893>
- Pokam, W. M., Djiotang, L. A. T., & Mkankam, F. K. (2012). Atmospheric water vapor transport and recycling in equatorial central Africa through NCEP/NCAR reanalysis data. *Climate Dynamics*, 38(9–10), 1715–1729. <https://doi.org/10.1007/s00382-011-1242-7>
- Richter, I., Chang, P., Doi, T., Kataoka, T., Nagura, M., Oettli, P., et al. (2016). An overview of coupled GCM biases in the tropics. In *Indo-Pacific Climate Variability and Predictability* (pp. 213–263). Texas: World Scientific. [https://doi.org/10.1142/9789814696623\\_0008](https://doi.org/10.1142/9789814696623_0008)
- Running, S. W., Mu, Q., Zhao, M., & Moreno, A. (2017). *User's guide: MODIS global terrestrial evapotranspiration (ET) product (NASA MOD16A2/A3): NASA Earth observing system MODIS land algorithm*. NASA: Washington DC, USA.
- Schmidt, G. A., Kelley, M., Nazarenko, L., Ruedy, R., Russell, G. L., Aleinov, I., et al. (2014). Configuration and assessment of the GISS ModelE2 contributions to the CMIP5 archive. *Journal of Advances in Modeling Earth Systems*, 6(1), 141–184. <https://doi.org/10.1002/2013MS000265>
- Schmidt, G. A., Ruedy, R., Hansen, J. E., Aleinov, I., Bell, N., Bauer, M., et al. (2006). Present-day atmospheric simulations using GISS ModelE: Comparison to in situ, satellite, and reanalysis data. *Journal of Climate*, 19(2), 153–192. <https://doi.org/10.1175/JCLI3612.1>
- Seneviratne, S. I., Corti, T., Davin, E. L., Hirschi, M., Jaeger, E. B., Lehner, I., et al. (2010). Investigating soil moisture-climate interactions in a changing climate: A review. *Earth-Science Reviews*, 99(3–4), 125–161. <https://doi.org/10.1016/j.earscirev.2010.02.004>
- Shevliakova, E., Pacala, S. W., Malyshev, S., Hurtt, G. C., Milly, P. C. D., Caspersen, J. P., et al. (2009). Carbon cycling under 300 years of land use change: Importance of the secondary vegetation sink. *Global Biogeochemical Cycles*, 23, GB2022. <https://doi.org/10.1029/2007GB003176>
- Sitch, S., Smith, B., Prentice, I. C., Arneth, A., Bondeau, A., Cramer, W., et al. (2003). Evaluation of ecosystem dynamics, plant geography and terrestrial carbon cycling in the LPJ dynamic global vegetation model. *Global Change Biology*, 9(2), 161–185. <https://doi.org/10.1046/j.1365-2486.2003.00569.x>
- Sjöström, M., Zhao, M., Archibald, S., Arneth, A., Cappelaere, B., Falk, U., et al. (2013). Evaluation of MODIS gross primary productivity for Africa using eddy covariance data. *Remote Sensing of Environment*, 131, 275–286. <https://doi.org/10.1016/j.rse.2012.12.023>
- Sonwa, D. J., Dieye, A., El Mzouri, E. H., Majule, A., Mugabe, F. T., Omolo, N., et al. (2017). Drivers of climate risk in African agriculture. *Climate and Development*, 9(5), 383–398. <https://doi.org/10.1080/17565529.2016.1167659>
- Sylla, M. B., Giorgi, F., Coppola, E., & Mariotti, L. (2013). Uncertainties in daily rainfall over Africa: Assessment of gridded observation products and evaluation of a regional climate model simulation. *International Journal of Climatology*, 33(7), 1805–1817. <https://doi.org/10.1002/joc.3551>
- Takata, K., Emori, S., & Watanabe, T. (2003). Development of the minimal advanced treatments of surface interaction and runoff. *Global and Planetary Change*, 38(1–2), 209–222. [https://doi.org/10.1016/S0921-8181\(03\)00030-4](https://doi.org/10.1016/S0921-8181(03)00030-4)
- Taylor, K. E., Stouffer, R. J., & Meehl, G. A. (2012). An overview of CMIP5 and the experiment design. *Bulletin of the American Meteorological Society*, 93(4), 485–498. <https://doi.org/10.1175/BAMS-D-11-00094.1>
- Trambauer, P., Dutra, E., Maskey, S., Werner, M., Pappenberger, F., Van Beek, L. P. H., & Uhlenbrook, S. (2014). Comparison of different evaporation estimates over the African continent. *Hydrology and Earth System Sciences*, 18(1), 193–212. <https://doi.org/10.5194/hess-18-193-2014>
- Verseghy, D. L. (2000). The Canadian land surface scheme (CLASS): Its history and future. *Atmosphere - Ocean*, 38(1), 1–13. <https://doi.org/10.1080/07055900.2000.9649637>
- Voldoire, A., Sanchez-Gomez, E., Salas y Mélia, D., Decharme, B., Cassou, C., Sénéci, S., et al. (2013). The CNRM-CM5.1 global climate model: Description and basic evaluation. *Climate Dynamics*, 40(9–10), 2091–2121. <https://doi.org/10.1007/s00382-011-1259-y>
- Volodin, E. M., Dianskii, N. A., & Gusev, A. V. (2010). Simulating present-day climate with the INMCM4.0 coupled model of the atmospheric and oceanic general circulations. *Izvestiya, Atmospheric and Oceanic Physics*, 46(4), 414–431. <https://doi.org/10.1134/S000143381004002X>
- Volodin, E. M., & Lykosov, V. N. (1998). Parameterization of heat and moisture transfer in the soil-vegetation system for use in atmospheric general circulation models: 1. Formulation and simulations based on local observational data. *Atmospheric and Oceanic Physics*, 34(4), 405–416.
- Von Salzen, K., Scinocca, J. F., McFarlane, N. A., Li, J., Cole, J. N. S., Plummer, D., et al. (2013). The Canadian fourth generation atmospheric global climate model (CanAM4). Part I: Representation of physical processes. *Atmosphere - Ocean*, 51(1), 104–125. <https://doi.org/10.1080/07055900.2012.755610>

- Wang, G., & Eltahir, E. A. B. (2000). Modeling the biosphere-atmosphere system: The impact of the subgrid variability in rainfall interception. *Journal of Climate*, 13(16), 2887–2899. [https://doi.org/10.1175/1520-0442\(2000\)013<2887:MTBAST>2.0.CO;2](https://doi.org/10.1175/1520-0442(2000)013<2887:MTBAST>2.0.CO;2)
- Wang, H. X., & Liu, C. M. (2007). Soil evaporation and its affecting factors under crop canopy. *Communications in Soil Science and Plant Analysis*, 38(1), 259–271. <https://doi.org/10.1080/00103620601094213>
- Washington, R., James, R., Pearce, H., Pokam, W. M., & Moufouma-Okia, W. (2013). Congo basin rainfall climatology: Can we believe the climate models? *Philosophical Transactions of the Royal Society B: Biological Sciences*, 368(1625), 20120296. <https://doi.org/10.1098/rstb.2012.0296>
- Watanabe, M., Suzuki, T., Oishi, R., Komuro, Y., Watanabe, S., Emori, S., et al. (2010). Improved climate simulation by MIROC5: Mean states, variability, and climate sensitivity. *Journal of Climate*, 23(23), 6312–6335. <https://doi.org/10.1175/2010JCLI3679.1>
- Webster, P. (1983). The large-scale structure of the tropical atmosphere. In *In General circulation of the atmosphere* (pp. 235–275). London: Academic Press.
- Wei, Z., Yoshimura, K., Wang, L., Miralles, D. G., Jasechko, S., & Lee, X. (2017). Revisiting the contribution of transpiration to global terrestrial evapotranspiration. *Geophysical Research Letters*, 44(6), 2792–2801. <https://doi.org/10.1002/2016GL072235>
- Whalley, W. R., Ober, E. S., & Jenkins, M. (2013). Measurement of the matric potential of soil water in the rhizosphere. *Journal of Experimental Botany*, 64(13), 3951–3963. <https://doi.org/10.1093/jxb/ert044>
- Wu, T., Song, L., Li, W., Wang, Z., Zhang, H., Xin, X., et al. (2014). An overview of BCC climate system model development and application for climate change studies. *Journal of Meteorological Research*, 28(1), 34–56. <https://doi.org/10.1007/s13351-014-3041-7>
- Xu, L., Saatchi, S. S., Shapiro, A., Meyer, V., Ferraz, A., Yang, Y., et al. (2017). Spatial distribution of carbon stored in forests of the Democratic Republic of Congo. *Scientific Reports*, 7(1), 15030. <https://doi.org/10.1038/s41598-017-15050-z>
- Yan, D., Zhang, X., Yu, Y., & Guo, W. (2017). Characterizing land cover impacts on the responses of land surface phenology to the rainy season in the Congo Basin. *Remote Sensing*, 9(5), 1–17. <https://doi.org/10.3390/rs9050461>
- Yu, M., Wang, G., & Chen, H. (2016). Quantifying the impacts of land surface schemes and dynamic vegetation on the model dependency of projected changes in surface energy and water budgets. *Journal of Advances in Modeling Earth Systems*, 8(1), 370–386. <https://doi.org/10.1002/2015MS000492>
- Zhao, M., Held, I. M., Lin, S. J., & Vecchi, G. A. (2009). Simulations of global hurricane climatology, interannual variability, and response to global warming using a 50-km resolution GCM. *Journal of Climate*, 22(24), 6653–6678. <https://doi.org/10.1175/2009JCLI3049.1>
- Zhou, L., Tian, Y., Myneni, R. B., Ciais, P., Saatchi, S., Liu, Y. Y., et al. (2014). Widespread decline of Congo rainforest greenness in the past decade. *Nature*, 509(7498), 86–90. <https://doi.org/10.1038/nature13265>
- Zhou, Z. Q., Xie, S. P., Zhang, G. J., & Zhou, W. (2018). Evaluating AMIP skill in simulating interannual variability over the Indo-western Pacific. *Journal of Climate*, 31(6), 2253–2265. <https://doi.org/10.1175/JCLI-D-17-0123.1>